Journal University of Kerbala , Vol. 16 No.4 Scientific . 2018

Experimental Study of Natural Convection Heat Transfer from Horizontal Cylinder with Circular, Elliptical, and Cusp Cross Sectional Area.

دراسة تجريبية لانتقال الحرارة بالحمل الحر من اسطوانة افقية ذات مساحة مقطعية (دائرية ، بيضوية ونتوئية)

M.Sc. Emad Esmaael Habib.
Mechanical Engineering Department - University of Technology - Baghdad-Iraq

Abstract:

Three copper cylinder oriented geometries have been experimentally tested for heat transfer enhancement. These geometries include ellipse, squared cusp and triangle cusp cross section. The circular cross section was also tested for comparison purposes. The test specimens have been manufactured using different machining processes such as lathing, riming, grinding and drilling. The test specimens were rotated around their centers by several angles 45°, 60° and 90° to obtain the optimum position for good heat transfer enhancement. The results reveals that the standing ellipse and square cusp have the high heat transfer coefficient. The circular cross section was found to have the lower value of heat transfer coefficient.

Key: Natural convection + horizontal cylinder + Geometry

الخلاصة :

تم اجراء الاختبارات التجريبية لثلاثة اشكال اسطوانية نحاسية وذلك لتحسين انتقال الحرارة . هذه المقاطع الهندسية تتضمن القطع الناقص و المربع والمثلث كما تم اختبار المقطع الدائري ايضا لاغراض المقارنة . تم تصنيع عينات الاختبار باستخدام عمليات تصنيع مختلفة مثل الخراطة والربط و الطحن والدرفلة .تم تدوير عينات الاختبار حول مركزها وبعدة زوايا هي(45 و 60 و 90) درجة وذلك للحصول على الوضع الامثل لتحسين انتقال الحرارة . بينت النتائج ان القطع الناقص والمربع امتاز بمعامل انتقال حرارة جيد في حين ان المقطع الدائري كان اقل قيمة لمعامل انتقال الحرارة.

Symbols	Definition	Units
As	Surface area	m^2
Bi	Biot number = hLc/k	
C_p	Specific heat	kJ/kg.K
d	Diameter	M
Gr	Grashof number	
h	Heat transfer coefficient	W/ m^2.K
hst	Steady state heat transfer coefficient	W/ m^2.K
hun	Un steady state heat transfer coefficient	W/ m^2.K
k	Thermal conductivity	W/ m.K
Lc	Characteristic length	m
Nu	Nusselt number	
Pr	Prandtl number	
Ra	Rayleigh number=Gr.Pr=$(\rho^2 g B \Delta T Lc^3/\mu^2).(\mu cp/k)$	
T∞	Ambient temperature	℃
Ts	Start temperature	℃
Te	End temperature	℃
t	Tim	sec
V	Volume	m^3
ρ	Density	kg/ m^3
β	Volume coefficient of expansion =1/(Ts+T∞)/2	1/K

- **Legend of Figures**

Figure (1) The exprimental apparatuse
Figure (2) Show the processes of the test rods.
Figure (3) The variation of body temperature and time for cylinder rod.
Figure (4) The variation of body temperature and time for ellipse horizontal rod.
Figure (5) The variation of body temperature and time for ellipse vertical rod.
Figure (6) The variation of body temperature and time for square cusp horizontal rod.
Figure (7) The variation of body temperature and time for square cusp vertical rod.
Figure (8) The variation of body temperature and time for triangle cusp horizontal rod.
Figure (9) The variation of body temperature and time for triangle cusp vertical rod.
Figure (10) The Biot number coefficient of different bodies.
Figure (11) The heat transfer coefficient of different bodies.
Figure (12) The Nusselt number of different bodies.

- **Introduction**

There are a number of practical applications of natural convection heat transfer from long horizontal circular and noncircular sections such as heat exchangers, solar collector design , heating and ventilation of building, nuclear , chemical reactors and cooling of electronic equipment.

Heat transfer enhancement using natural convection was the subject of many researches in recent years. In view of power consumption and economical consideration an experimental study of natural convection was carried by Alayilmaz and Teke [1] on a horizontal cylinder. They claimed that although the subject has been studies extensively over the last 50 years, discrepancies still obtained in the output data of the prior researches due to various factors. Churchill and chu [2] published an article on laminar and turbulent natural convection from horizontal cylinder. For the laminar regime, they took the limiting Nu expression of Savill and Churchill [3] and used a form suggested by Churchill and Usagi [4] and Tsubouchi and Masuda [5] in order to obtain an expression to the average Nusselt number for the horizontal cylinder of circular cross section for

$2.3 \times 10^4 \leq Gr \leq 7.5\times10^4$:

$Nu_D = 0.44\, Gr^{0.25}$

Fujii et al [6] performed an analytical and experimental study on a horizontal platinum wire of 0.47 mm diameter and 238 mm long situated in air stream.

Xing Yuan [7] studied free convection in a horizontal concentric annuli with different inner shapes. The simulation is categorized into four groups based on the shape of the inner entity which can be either cylindrical, elliptical, square or triangular. Overall heat transfer correlations incorporating thermal radiation are established and presented in terms of the Nusselt numbers. It is observed that the surface radiation and existence of the corners and larger top space can enhance the heat transfer rate. As the reference temperature and Rayleigh number increases, surface radiation plays a more prominent role in the overall heat transfer performance.

The aim of the research is to find the heat transfer coefficients of these different shapes and compare their results. The triangular cusp shape and the diamond cusp shape are investigated for the first time up to our knowledge.

- **Testing apparatus:**

The apparatus consist of a Perspex section with (200x150x150) mm, with holes in one of its faces to insert the copper rods inside it as shown in Figure (1). The rods made of copper with length of 126 mm with different cross sectional area (circular, ellipse, square cusp, and triangle cusp). These test specimens have been manufactured using several operational processes; lathing, riming, grinding and drilling as shown in Figure (2).the elliptic section was oriented as standing position. Two orientation were tested for each geometry as shown in Figures (4-9). To heating the rods the apparatus consist of electric heating element like cylinder with hole in the center to insert the rod. The maximum allowable temperature is around 85 °C. Electrical power input had been used to heat up the specimen until the temperature became 80 ℃.

Each rod has a hole in its center to fix a thermistor to measure the temperature variation with time when the rod inserted in the test section. The test of each specimen carried out alone in the system to find the test results. The first thermistor which inserted inside the bore of the rod connected into Labjack interface to measure the section temperature variation. The interface connected to laptop and by Labjack software reads the variation of the rods temperature and section temperature simultaneously with time. The thermistor had fast response time to measure the temperature variation. The temperature measuring time duration was between (10-20) seconds. The accuracy of temperature measuring is ∓0.1℃ according to the manufacturing data. The outside temperature during the tests of specimens was 41℃ because it was summer time and the space was unconditioned.

- **Lumped Thermal Capacity Model**

The first method that used to analyze the experimental data is the Lumped thermal capacity model which assume that partial temperature variations within the body are negligible and the temperature variation is only a function of time [8]. The geometry of cylinder, ellipse, square cusp, triangle cusp of volume *V,* surface area *As,* density ρ, and specific heat c_p, initially at a temperature *Ts* were selected. At time $t \geq 0$, the body is immersed in a convective environment (T_∞, h), where $T_\infty < Ts$, and allowed to cool. The equation describing the cooling process is

$$\rho V c_p \frac{dT}{dt} = -hA_s\,(T - T_\infty)$$

With the initial condition $T(t=0) = T_s$

The solution is:

$$\frac{T_e - T_\infty}{T_s - T_\infty} = e^{-hA_s\,t/\rho V c_p} \quad \text{or}$$

$$ln\frac{T_e - T_\infty}{T_s - T_\infty} = -\frac{hA_s\,t}{\rho V c_p} \qquad \text{----------------(1)}$$

h = heat transfer coefficient (W/m^2.K)

The lumped thermal capacity model is valid for $B_{i=}\frac{hL_c}{k} < 0.1$.

- **Steady State Model:**

The second method to analyze the behavior of thermal system by using empirical equation for natural convection to find the heat transfer coefficient for the horizontal cylinder [9]:

$$h = 1.32(\Delta T/d)^{\frac{1}{4}} \quad \text{For} \quad 10^4 < R_a < 10^9 \qquad \text{----------------(2)}$$

where:

$$R_a = G_r.P_r = \frac{g\beta(\Delta T)\rho^2 L_c^3}{\mu^2}.\frac{\mu\,C_p}{k}$$

The value of the heat transfer coefficient *h* was calculated using equation (1) and (2) with the help of the experimental data for the temperature variations of the tested geometries. The results were plotted as surface temperature variation with time, heat transfer coefficient, *Nu* and *Bi*, as shown in next section. The value of Rayleigh number was calculated and found to be around 3-4x10^6 which is in the range of equation (2).

- **Results and discussion:**

Figure (3-9) show the temperature decreasing with time for each rod, the decreasing behavior identical to a negative exponential decay. These figures specify the relationship between temperature variations of different rods with time. The initial and final temperature can be seen for each type in figures. The temperature decrease with time for each rod, the decreasing behavior identical to a negative exponential decay within a certain time shown in figures. It can be noticed that the Biot number is less than 0.1 as shown in Figure (10). Therefor the Lump thermal capacity analysis can be applied. Figure (11) show the magnitude of heat transfer coefficient for each rod by using the unsteady state method (lumped thermal capacity method) and steady state method.

The values of Bi, Ra, Nu and h are listed in Table (1) below for each type of the rods mentioned.

The magnitude of the heat transfer coefficient at unsteady state higher than its steady state value by ≅ 10.2%. The cylindrical rod had the lower heat transfer coefficient value while the vertical cusp square had the higher value. The cusp shape gave the higher value of the heat transfer coefficient because of the enhancement in the buoyancy effect. The curved surface area has also partially increased the heat transfer rates in the cusp section which leads to the increase in the heat transfer coefficient value. Figure 12 shows the Nusselt number variation of seven geometries. The maximum value was found to be for the standing square cusp which is follow the values of the heat transfer coefficient as seen in figure 11. However this may be attributed to geometrical and orientation causes. The first one is the buoyancy current on the lower curved surfaces as it moves upward create two separated blumes while the two upper curved surfaces create one single blume. These three blumes enhance the heat exchange with the surrounding better than the other geometry.

Table (1) The experimental

No	Name	Bi	Ra	Nu	h
1	Square cusp vertical	0.004631	4.448E6	66.08	14.6
2	Ellipse vertical	0.004379	3.224E6	62.5	13.69
3	Ellipse horizontal	0.004295	3.224E6	61.29	13.43
4	Triangular cusp vertical	0.004258	3.2443E6	60.81	13.32
5	Square cusp horizontal	0.004208	4.591E6	59.97	13.26
6	Triangular cusp horizontal	0.004095	2.846E6	58.82	12.81
7	Circular	0.00348	3.608E6	49.63	10.8

- **Conclusion**

Three copper cylinders of different geometries were experimentally tested for heat transfer coefficient enhancement. The test specimens were of ellipse, squared cusps and triangular cusp cross sections. During tests these specimens were rotated for 45^o, 60^o and 90^o as required to examine the optimum position for good convection heat transfer coefficient. It was concluded that the standing square cusp copper rod has the highest heat transfer coefficient of (14.6 W/m^2.K) while the conventional circular cross section rod was found to has the lowest value of heat transfer coefficient of (10.8 $W/m^2.K$). This suggests that the cusp shape has a good effect in enhancing the heat transfer from curved surfaces.

•References:

[1] Atayilmaz ¸SÖ, Teke I (2009) Experimental and numerical study of the natural convection from a heated horizontal cylinder. Int Commun Heat Mass 36:731–738

[2] Churchill SW, Chu HHS (1975) Correlating equations for laminar and turbulent free convection from a vertical plate. Int J Heat Mass Transfer 18:1323–1329

[3] Saville D, Churchill S (1967) laminar free convection in boundary layers near horizontal cylinders and vertical axisymmetric bodies. J Fluid Mech 29:391–399

[4] Churchill S, Usagi R (1972) A general expression for the correlation of rates of transfer and other phenomena. AICHE J 18:1121–1128

[5] TsubouchiT, MasudaH(1966–1967) Natural convection heat transfer from a horizontal circular cylinder with small rectangular grooves. Sci Rep Res Inst Tohaku Univ Ser B 18:211–242

[6] Fujii T, Fujii M, Honda T (1982) Theoretical and experimental studies of the free convection around a long horizontal thin wire in air. In: Proceedings of the 7th international heat transfer conference, vol 6. Munich, Germany, pp 311–316.

[7] Xing Yuan (2014) An Investigation of Natural Convection in a Horizontal Concentric Annuli With Different Inner Shapes. Thesis, University of California

[8] YUNUS A. CENGEL, Heat transfer, second edition, 2008.

[9] J.P.Holman, heat transfer, ten edition, 2010.

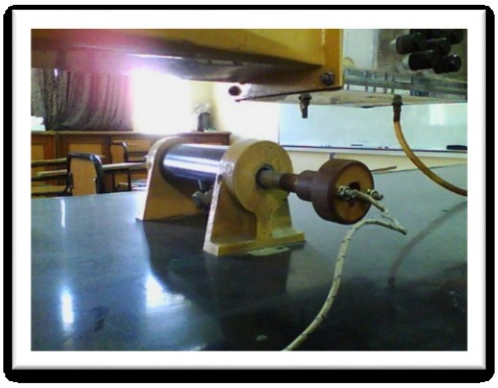

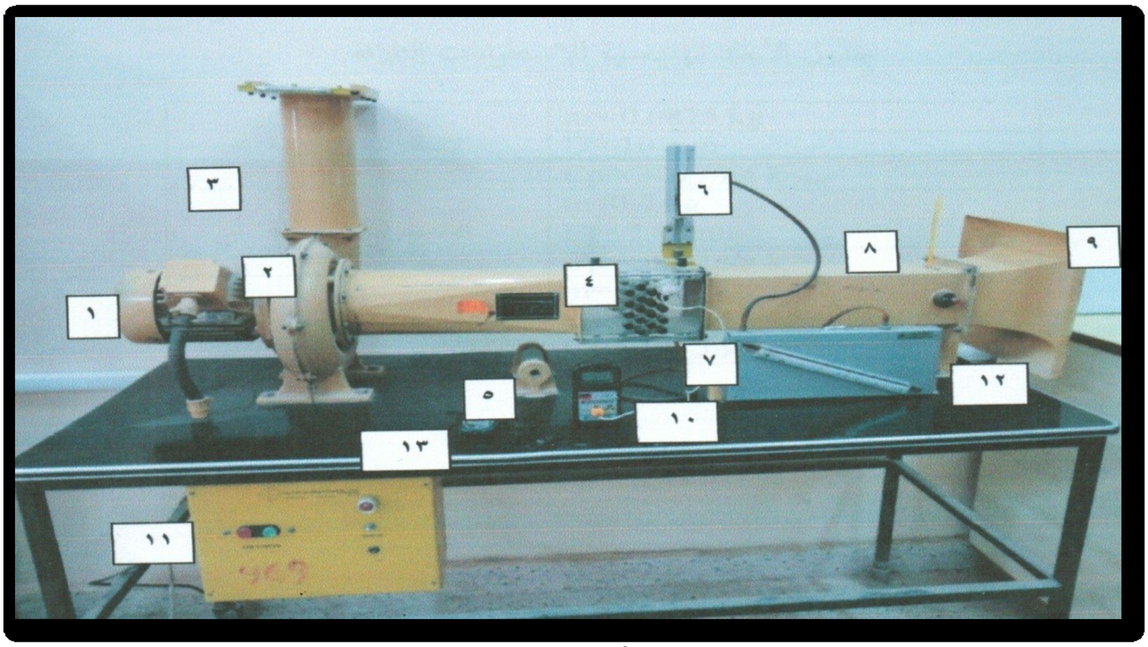

1	Electric motor	6	Total head tube	11	Control panel
2	Fan	7	Test element	12	Inclined manometer
3	Throttle opening	8	Thermometer	13	Watch time
4	Working section	9	Air inlet		
5	Electric heater	10	Digital thermometer		

Figure (1) The exprimental apparatuse

Figure (2) Show the processes of the test rods.

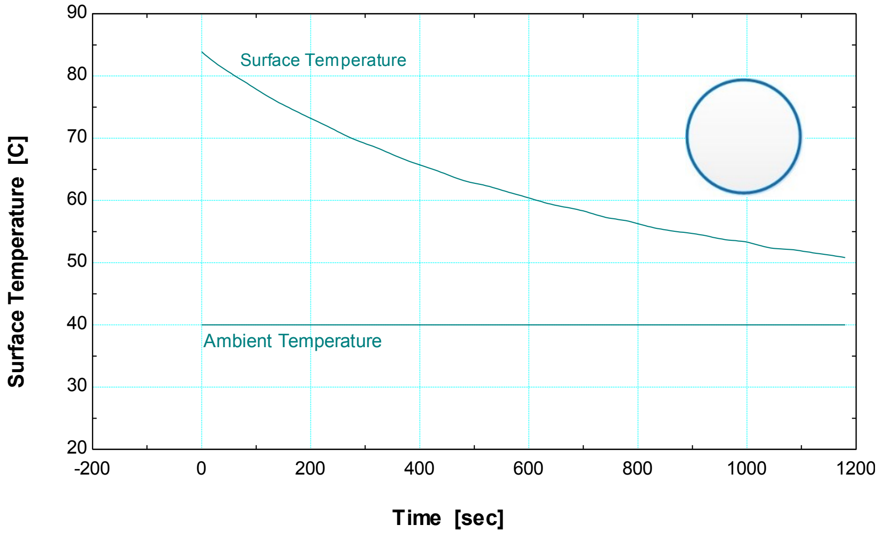

Figure (3) The variation of body temperature and time for cylinder

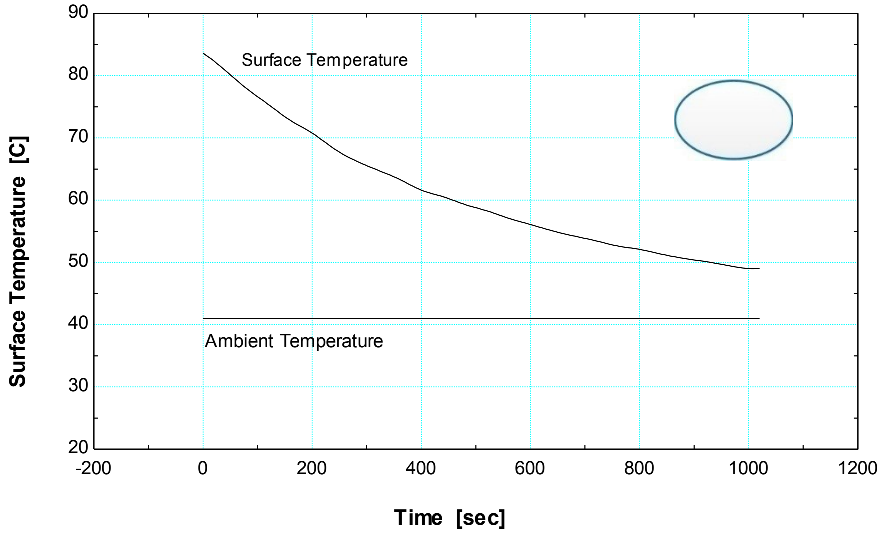

Figure (4) The variation of body temperature and time for ellipse horizontal rod.

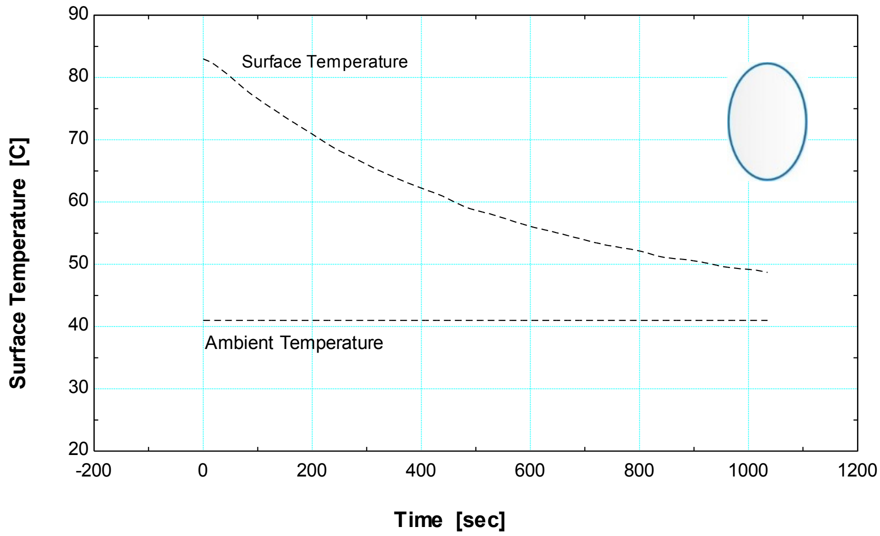

Figure (5) The variation of body temperature and time for ellipse vertical

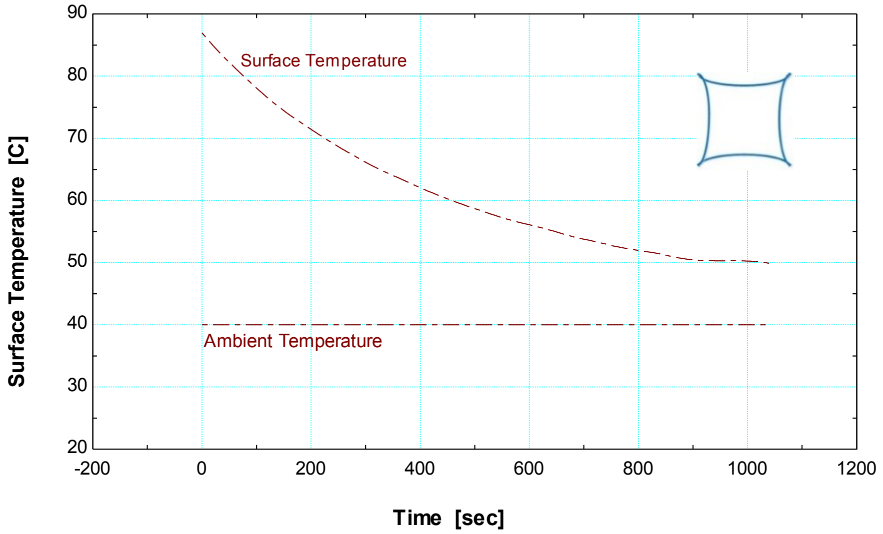

Figure (6) The variation of body temperature and time for square cusp

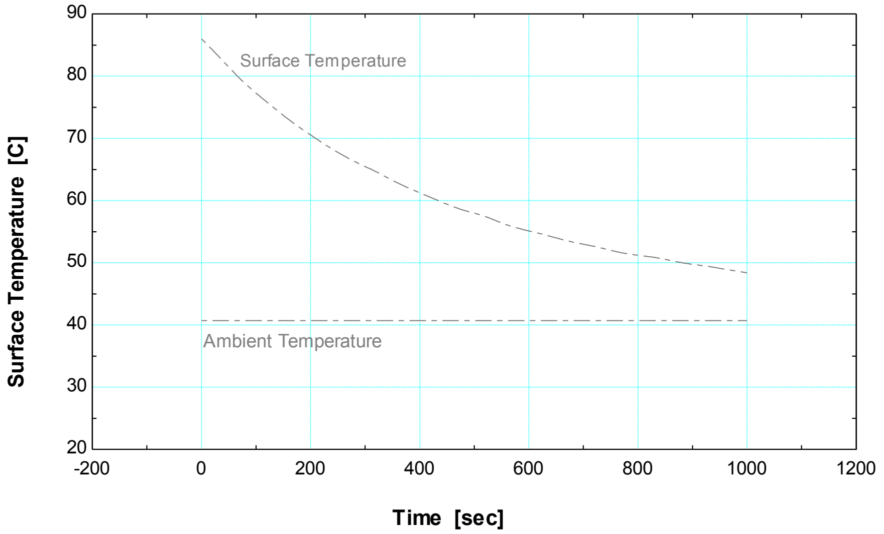

Figure (7) The variation of body temperature and time for square cusp vertical rod.

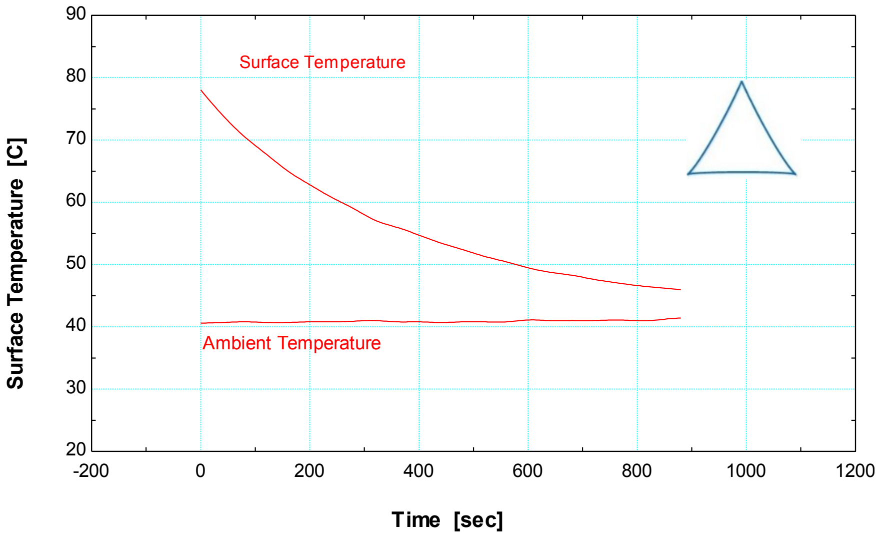

Figure (8) The variation of body temperature and time for triangle cusp horizontal rod.

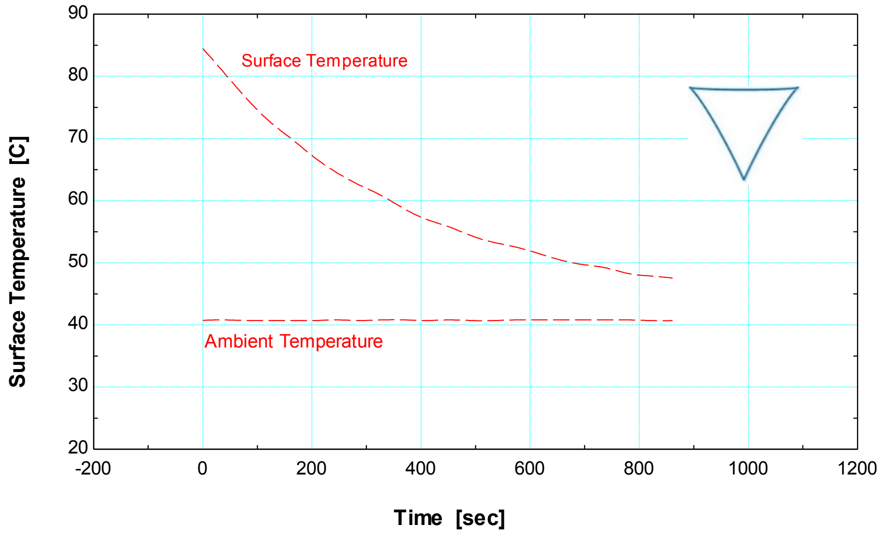

Figure (9) The variation of body temperature and time for triangle cusp vertical rod.

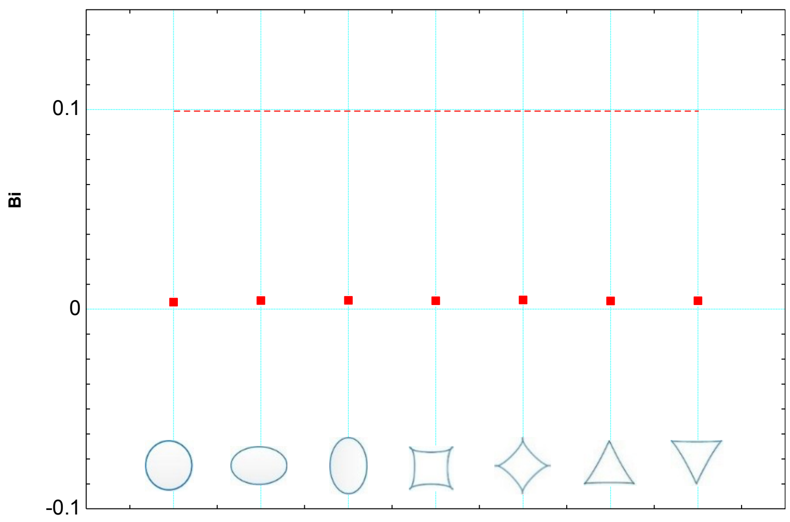

Figure (10) The Biot number coefficient of different

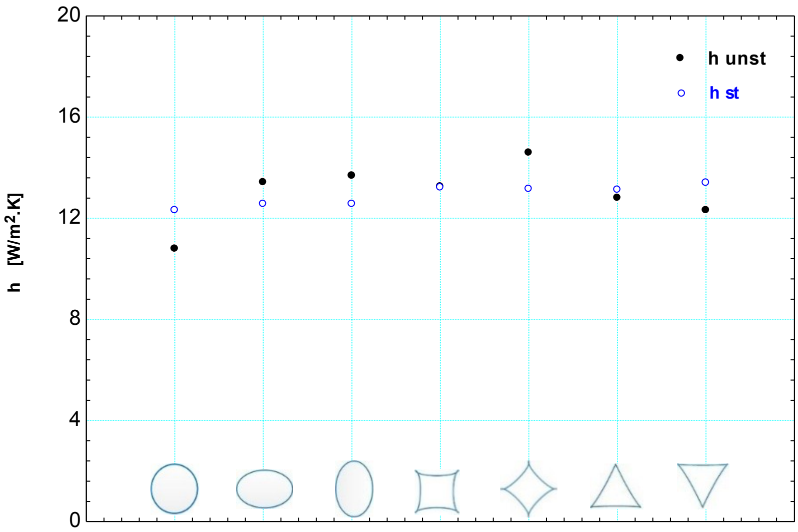

Figure (11) The heat transfer coefficient of different

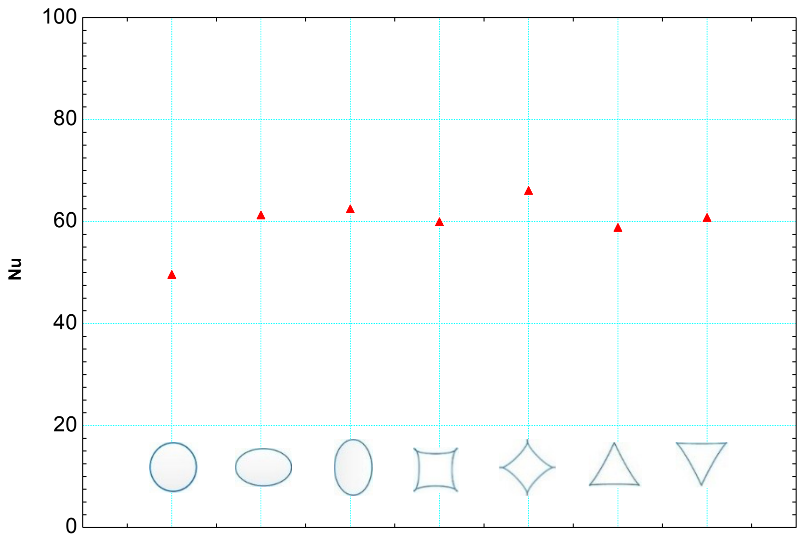

Figure (12) The Nusselt number of different bodies.